Macromolecules
ARTICLE

Macromolecules **2010**, *43*, 7577–7582 **7577**
DOI: 10.1021/ma101468r

High Surface Area Contorted Conjugated Microporous Polymers Based on Spiro-Bipropylenedioxythiophene

Jia-Xing Jiang, Andrea Laybourn, Rob Clowes, Yaroslav Z. Khimyak, John Bacsa, Simon J. Higgins, Dave J. Adams, and Andrew I. Cooper*

Department of Chemistry and Centre for Materials Discovery, Crown Street, University of Liverpool, Liverpool L69 3BX, U.K.

Received July 1, 2010; Revised Manuscript Received August 10, 2010

ABSTRACT: Conjugated polymers derived from thiophene or 3,4-ethylenedioxythiophene derivatives have been widely investigated for use in organic thin-film transistors and organic photovoltaic devices. We describe here the synthesis of a series of conjugated microporous polymers formed by reaction of spiro-bis(2,5-dibromopropylenedioxythiophene) with one of three di- or triethynyl monomers. These polymers have surface areas up to 1631 m^2/g and exhibit significant microporosity, suggesting possible applications in the fields of organic electronics or optoelectronics.

Introduction

Microporous organic polymers are attracting increasing attention due to their potential applications in areas such as gas adsorption, separation, and heterogeneous catalysis.[1,2] In recent years, these applications have inspired the synthesis of a wide variety of microporous organic polymers including polymers of intrinsic microporosity (PIMs),[3−6] hyper-cross-linked polymers (HCPs),[7−9] covalent triazine-based frameworks (CTFs),[10] covalent organic frameworks (COFs),[11,12] polyanilines,[13] and polyimides.[14,15] In 2007, we reported the first synthesis of a conjugated microporous polymer (CMP).[16] These poly(aryleneethynylene)s (PAEs) networks showed apparent Brunauer−Emmett−Teller (BET) surface areas (S_{BET}) of up to 834 m^2/g and, subsequently, more than 1000 m^2/g.[17] A number of other examples of CMPs (or closely related structures) have since been synthesized using various chemical strategies.[18] For example, we reported alkyne−alkyne homocoupling as a route to conjugated microporous/mesoporous poly(phenylene butadiynylene)s (HCMPs) (S_{BET} = 840 m^2/g).[19] We also demonstrated the synthesis of a mesoporous poly(phenylenevinylene) (PPV) network with S_{BET} of 761 m^2/g using the Gilch reaction.[20] Thomas et al.[21] described both microporous poly(*p*-phenylene) and poly(phenyleneethynylene) materials based on a spirobifluorene building block (S_{BET} = 450−510 m^2/g) by Suzuki or Sonogashira−Hagihara cross-coupling chemistry. The same group synthesized conjugated microporous poly(thienylenearylene) networks[22] using oxidative polymerization of multiple thiophene-functionalized structure directing motifs. Kobayashi and co-workers have described the indirect preparation of pyrolytic conjugated porous polymers via heat treatment of alkyl-substituted poly(phenylenevinylene) precursors at high temperatures (> 350 °C).[23] Other related studies have shown that CMPs can be prepared by Yamamoto polymerization.[24] Following this, Ben et al.[25] synthesized a microporous polyphenylene network by Yamamoto polymerization, PAF-1, which is reported to have unprecedented surface area (S_{BET} = 5640 m^2/g).[26] Despite this significant progress, there is still a need to broaden the range of chemical functionality which can be incorporated into CMPs with high surface area in order to enable new applications which exploit the conjugated nature of these materials.[27] For example, we recently demonstrated that it is possible to cross-couple monomers with a range of different functional groups by Sonogashira−Hagihara coupling,[28] allowing us to prepare polymers with high surface area and tailored physical properties. Following this, we have been interested in incorporating other functional groups into these networks.

Conjugated polymers derived from thiophene or 3,4-ethylenedioxythiophene derivatives have been widely investigated for use in organic thin-film transistors[29] and organic photovoltaic devices.[30] The synthesis of a 3-dimensional polymer network based on 3,4-ethylenedioxythiophene derivatives by electropolymerization has also been reported, although the porosity of the resulting network was not measured.[31] Polymers in this class have unusually low oxidation potentials,[32,33] and hence one could achieve second-generation materials with novel properties via the introduction of microporosity. For example, such materials may be of interest for sensors where high surface areas available may be of particular benefit. We describe here a series of contorted conjugated microporous polymer networks based on a novel monomer (spiro-bis(2,5-dibromopropylenedioxythiophene)) via Pd-catalyzed Sonogashira−Hagihara cross-coupling chemistry. The polymers show enhanced surface areas (up to 1631 m^2/g) and exhibit a reversible adsorption of up to 1.71 wt % hydrogen at 1.13 bar/77 K. These polymers might open up new possibilities for applications in the field of organic electronics or optoelectronic compounds.

Experimental Section

Chemicals. 1,3,5-Triethynylbenzene was purchased from ABCR. 1,4-Diethynylbenzene, tris(4-bromophenyl)amine, trimethylsilylacetylene, dichlorobis(triphenylphosphine)palladium(II), tetrakis(triphenylphosphine)palladium(0), copper(I) iodide, *N*-bromosuccinimide, and other chemicals and solvents were all purchased from Aldrich and either recrystallized or used as-received.

Synthesis of Spiro-Bipropylenedioxythiophene (1). Monomer **1** was synthesized using literature procedures.[34] Anal. Calcd for $C_{13}H_{12}O_4S_2$: C, 52.69; H, 4.08. Found: C, 52.63; H, 4.06. ^{1}H NMR ($CDCl_3$) δ (ppm): 6.49 (s, 4H), 4.05 (s, 8H). ^{13}C NMR ($CDCl_3$) δ (ppm): 148.85, 105.20, 71.19, 50.45.

Synthesis of Spiro-Bis(2,5-dibromopropylenedioxythiophene) (2). *N*-Bromosuccinimide (2.0 g, 11.25 mmol) in DMF (40 mL)

*To whom correspondence should be addressed.

Published on Web 08/17/2010

Scheme 1. Synthetic Routes to the Monomer 2 and the Polymers SPT-CMP1 to SPT-CMP3[a]

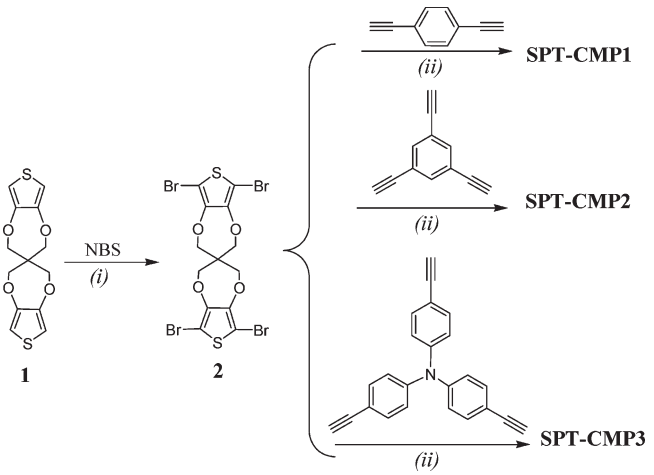

[a] Reagents and conditions: (i) $CHCl_3$ and DMF, RT for 6 h; (ii) $Pd(PPh_3)_4$, CuI, DMF, and Et_3N, 90 °C for 72 h.

was added to a solution of **1** (740 mg, 2.5 mmol) in $CHCl_3$ (50 mL) over 45 min. The mixture was stirred at room temperature for 6 h and then concentrated under reduced pressure. Water (200 mL) was added into the residue with stirring. The precipitate was filtered and washed with water and methanol, and the crude product was purified by recrystallization from THF/MeOH (1/3, v/v) to give **2** as a white crystalline solid (1.2 g, 76%). Anal. Calcd for $C_{13}H_8O_4Br_4S_2$: C, 25.52; H, 1.32. Found: C, 25.42; H, 1.35. ^{1}H NMR ($CDCl_3$) δ (ppm): 4.13 (s, 8H). ^{13}C NMR ($CDCl_3$) δ (ppm): 146.07, 91.33, 71.03, 50.84.

Synthesis of Tris(4-ethynylphenyl)amine. To a solution of tris-(4-bromophenyl)amine (4.82 g, 10.0 mmol), copper(I) iodide (57 mg, 0.3 mmol), and dichlorobis(triphenylphosphine)palladium-(II) (210 mg, 0.3 mmol) in diethylamine (40 mL) was added trimethylsilylacetylene (2.95 g, 30.0 mmol) dropwise under a nitrogen atmosphere. The mixture was heated to 50 °C and stirred for 12 h. After cooling to room temperature, the precipitate formed was collected by filtration and washed with diethyl ether. The combined filtrates were evaporated under reduced pressure, and the crude product was purified by column chromatography (silica gel, light petroleum) to give tris(4-trimethylsilylethynyl)-phenylamine as an intermediate. Hydrolysis of this compound was carried out directly by treatment with a mixture of MeOH (50 mL)/NaOH (50 mL, 1 M) with stirring at room temperature for 12 h. Standard work-up involved evaporation of the organic solvent, extraction of the residue with ether, drying with Mg_2SO_4 overnight, and removal of the solvent under reduced pressure. The crude product was purified by column chromatography (silica gel, light petroleum) to give tris(4-ethynylphenyl)amine as a white solid (yield: 2.5 g, 79%). Anal. Calcd for $C_{24}H_{15}N$: C, 90.85; H, 4.73; N, 4.42. Found: C, 90.47; H, 4.69; N, 4.38. Mass *m*/*z*: 335.24 $[M + NH_4]^+$. ^{1}H NMR ($CDCl_3$) δ (ppm): 7.35 (d, 6H), 6.47 (d, 6H), 3.15 (s, 3H). ^{13}C NMR ($CDCl_3$) δ (ppm): 140.75, 133.26, 123.45, 118.24, 83.47. 78.26.

Synthesis of Polymer Networks by Sonogashira−Hagihara Cross-Coupling Chemistry. All polymerization reactions were carried out at a fixed total molar monomer concentration (400 mmol/L) and a fixed reaction temperature and reaction time (90 °C/72 h). The molar ratio of ethynyl to bromine functionalities in the monomer feed was set at 1.5:1 based on our previous findings for CMP networks.[16,17] A representative experimental procedure for SPT-CMP1 is given as an example.

SPT-CMP1. 1,4-Diethynylbenzene (190 mg, 1.5 mmol), monomer **2** (306 mg, 0.5 mmol), tetrakis(triphenylphosphine)palladium-(0) (15 mg), and copper(I) iodide (10 mg) were dissolved in the mixture of DMF (2.5 mL) and Et_3N (2.5 mL). The reaction mixture was heated to 90 °C and stirred for 72 h under a nitrogen atmosphere

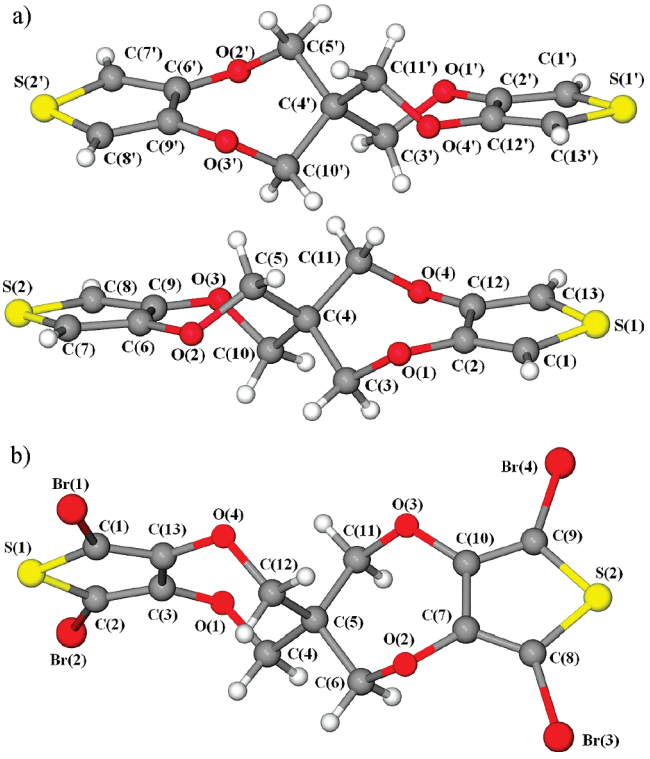

Figure 1. Single crystal X-ray structures of **1** (a) and monomer **2** (b).

(in order to rigorously exclude oxygen and to prevent any homocoupling of the alkyne monomers). The mixture was cooled to room temperature, and the insoluble precipitated network polymer was filtered and washed four times with chloroform, water, methanol, and acetone to remove any unreacted monomers or catalyst residues. Further purification of the polymer was carried out by Soxhlet extraction with methanol for 24 h. The product was then dried under vacuum for 24 h at 70 °C to give brown powder (yield: 204 mg, 75.4%). FT-IR (KBr cm^{-1}): 3300.5 (−C≡C−H), 2201.7 (−C≡C−). Elemental combustion analysis (%) Calcd for $C_{33}H_{16}O_4S_2$: C 73.32, H 2.98, S 11.86, O 11.84. Found: C 71.49, H 3.30. The main reason for the deviation of the elemental analysis from that expected is unreacted alkyne and bromo end groups and the catalyst residues found by EDX.[35]

Results and Discussion

The general synthetic routes to monomer **2** and the three polymer networks are shown in Scheme 1. Monomer **2**, a novel 3,4-ethylenedioxythiophene derivative, was prepared by bromination of spiro-bipropylenedioxythiophene (**1**) with *N*-bromosuccinimide (NBS) at room temperature. The absence of the thiophene proton in the ^{1}H NMR spectrum of monomer **2** indicates that the bromination reaction was successful (Supporting Information, Figures S1 and S3). The single crystal X-ray structure for **1** is shown in Figure 1a. There are two molecules in the asymmetric unit ($Z' = 2$), and the two molecules are near perfect mirror images of each other. Each molecule in the unit cell is chiral due to a helical twist through the molecular axis, and the two thiophene rings are not quite coplanar; the dihedral angle between the least-squares planes of the thiophene rings is 12.7(4)°. This contrasts with a previously determined X-ray structure of spiro-bipropylenedioxythiophene in which the two thiophene rings, oxygen atoms, and the spiro carbon are all in the same plane.[34] This implies that the spiro unit in **1** is flexible and can adopt a planar configuration if the crystal packing forces are suitable. On the other hand, the single crystal X-ray structure of monomer **2**, as seen in Figure 1b, shows that the molecule is highly twisted based on the spiro carbon

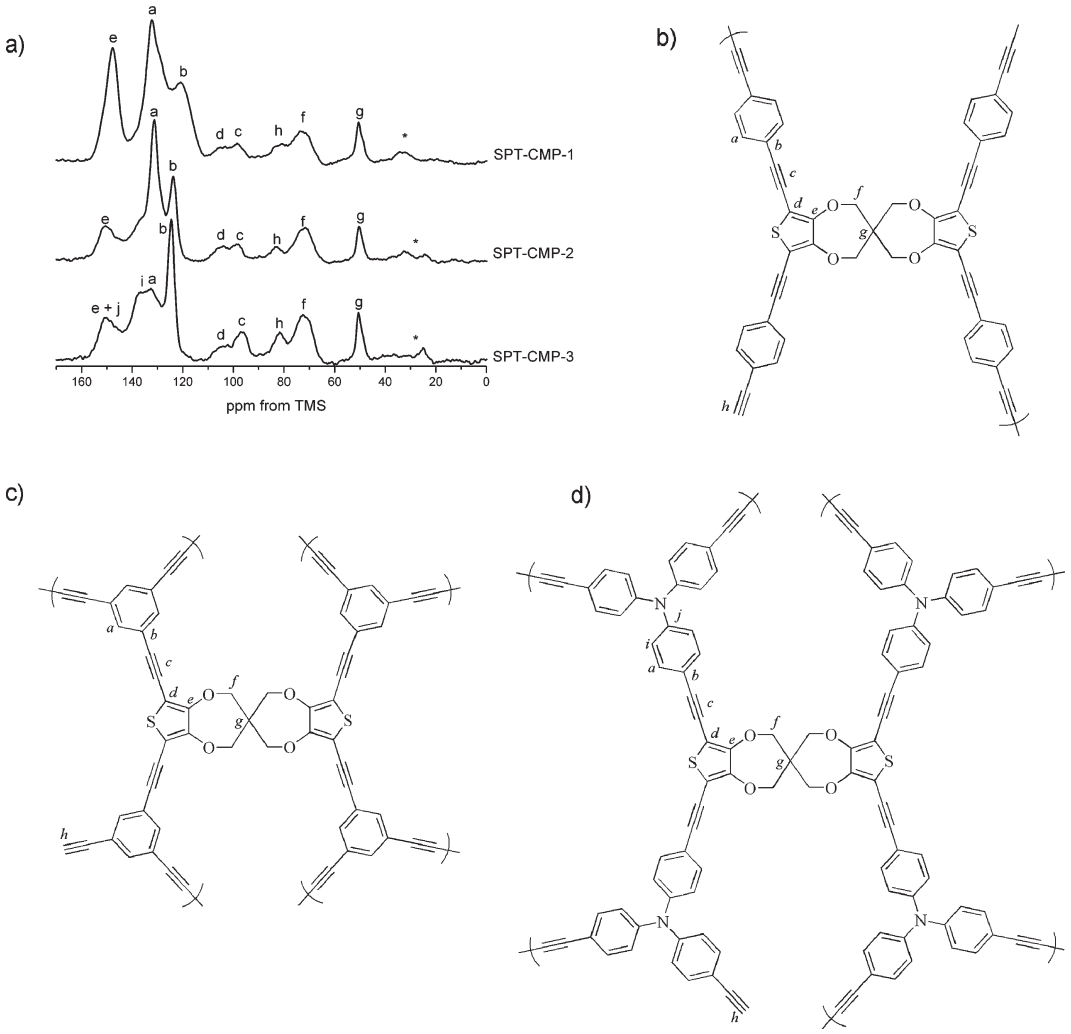

Figure 2. (a) Solid-state $^{1}H-^{13}C$ CP/MAS NMR spectra for SPT-CMP networks recorded at a MAS rate of 10 kHz. Asterisks denote spinning sidebands. (b) Representative molecular structure of the repeat units for SPT-CMP1, (c) for SPT-CMP2, and (d) for SPT-CMP3.

center and the two thiophene rings are not coplanar. The dihedral angle between the least-squares planes of the thiophene rings is 82.7 (±2)°.

The polymer networks were synthesized by using Sonogashira–Hagihara cross-coupling with a 1.5:1 molar ratio of ethynyl to bromine functionalities in DMF.[17] The reason for this monomer ratio giving rise to higher surface area materials is not clear although this tendency has been found for a range of systems and was reported in detail in previous studies.[17] We speculate the effect could be due to solubility effects as the polymerization takes place—for example, ethynl-capped oligomers might phase separate slightly later in the reaction. Alternatively, it could be that the effective reactive functionality for the 1,3,5-triethynylbenzene monomer is somewhat less than the idealized value of three as a result of the sterically constrained reaction environment in the rigid, cross-linked network. For example, it is possible that network growth continues in a heterogeneous fashion after early onset phase separation in the reaction mixture and that there are occluded and unreactive ethynl groups in the growing polymer network.

It was found that higher surface areas can be obtained by using DMF instead of toluene for the polymerization. The marked effect of solvent choice on the final porosity of a broader range of polymers will be published elsewhere. The polymer networks are not soluble in common solvents such as THF, toluene, DMF, and chloroform and are chemically stable. Moreover, the work-up conditions (> 48 h Soxhlet extraction, MeOH) did not significantly reduce porosity or surface area with respect to materials purified by simple washing.

The polymers were characterized at the molecular level by $^{1}H-^{13}C$ CP/MAS NMR in order to confirm the structures of the polymer networks (Figure 2), since it is also possible in principle to form homocoupled polybutadiynylene networks from alkyne–alkyne reactions in cases where the bromo-functionalized monomers are not sufficiently reactive or if conditions are insufficiently anaerobic.[19,28] The incorporation of the spiro-bipropylenedioxythiophene units results in overlapping of peaks in the $^{1}H-^{13}C$ CP/MAS NMR spectra, thus making the assignment of the resonances more difficult than for previous classes of CMPs. However, the resonances due to the spiro-bipropylenedioxythiophene units were easily distinguished by the sharp spiro carbon peak at ca. 50 ppm and the methylene carbon peak at ca. 71 ppm, indicating that the cross-coupling reaction had occurred and that the products were not simply the result of homocoupling of the alkyne monomers.[19,28] All SPT-CMP polymer networks show aromatic peaks at ca. 132 ppm ($\mathbf{C}_{ar\text{-}H}$) and 124 ppm ($\mathbf{C}_{ar}-C\equiv C-$) and the quaternary alkyne Car–$\mathbf{C}\equiv\mathbf{C}$–Car units peak at ca. 90 ppm, which are consistent with those of CMPs synthesized previously.[16,17] The peaks at ca. 82 ppm can be ascribed to the unreacted $-C\equiv\mathbf{C}H$ end groups. Their content was higher than that observed for CMPs synthesized previously.[16,17,35] We observed previously the halogenated end group at ca. 137 ppm for the protonated carbons of aromatic end

Table 1. Peak Assignments Corresponding to the $^{1}H-^{13}C$ CP/MAS NMR Spectra[a]

network	a	b	c	d	e	f	g	h	i	j	ratio[b]
SPT-CMP1	132.5	124.5	96.9	104.9	150.1	72.6	50.6	81.7			1.07
SPT-CMP2	131.2	123.7	98.7	104.5	150.3	71.6	50.3	82.7			1.30
SPT-CMP3	132.4	124.4	95.7	104.3	149.6	71.8	50.0	81.6	136.6	149.6	1.57

[a] All data in ppm. [b] Ratio of integration of terminal alkyne:quaternary alkyne.

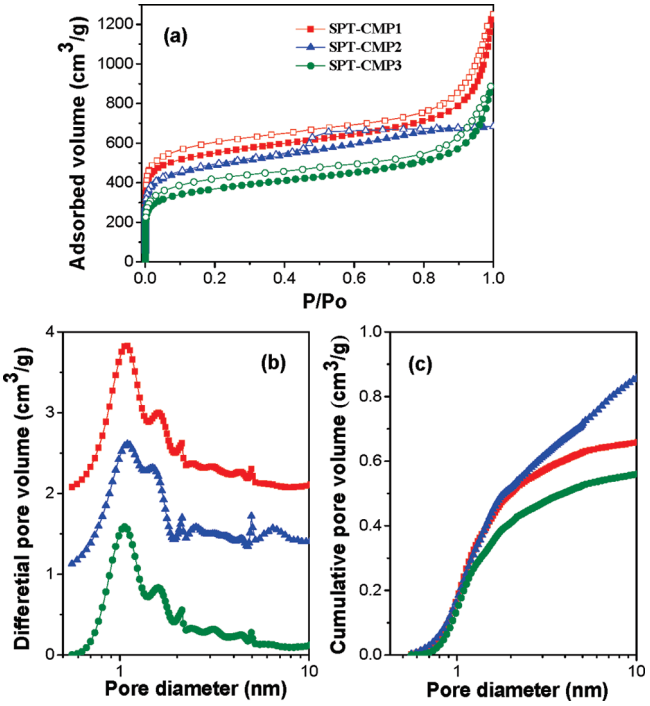

Figure 3. (a) N_2 adsorption−desorption isotherms measured at 77.3 K (adsorption branch is labeled with filled symbols and desorption is labeled with empty); for clarity, the isotherms of SPT-CMP1 and SPT-CMP2 were shifted vertically by 100 and 50 cm^3/g, respectively. (b) Pore size distribution curves; for clarity, the curves of SPT-CMP1 and SPT-CMP2 were shifted vertically by 2 and 1 cm^3/g, respectively. (c) Cumulative pore volume curves calculated by application of NL-DFT.

groups bearing residual iodine atoms for previous CMPs;[16] however, the terminal thiophene-Br end groups here would be expected at ca. 87 ppm, and it is possible that thiophene-Br and alkyne groups may overlap in the NMR spectrum, which leads to a higher intensity in the alkyne region than observed for other CMPs.[16] CP kinetics experiments were used to assign the peaks (Table 1) and also to help in the identification of possible bromine end groups (see Supporting Information, Figure S5 and Table S1). However, it is difficult to distinguish from these data whether the carbons resonating in this region are brominated. The degree of polycondensation for the networks can be estimated using the ratio of terminal alkyne to quaternary alkyne, using spectral deconvolution in the alkyne region[28] (see Supporting Information, Figures S6−S8). It was found that all of the SPT-CMP networks have lower degree of polycondensation (as shown by the ratio of terminal alkyne to quaternary alkyne, Table 1) than that of a number of previous CMP networks (where the ratio never exceeded 0.8),[28] suggesting that the SPT-CMP networks preferentially terminate at the alkyne functionality.

The porosity of the polymer networks was investigated by sorption analysis using N_2 and H_2 as the sorbate molecules. Figure 3a shows the N_2 adsorption and desorption isotherms for the resulting polymers. The three polymer networks gave rise to type I nitrogen gas sorption isotherms with H3 hysteresis loops, indicating that the materials consist of micro- and mesopores. Somewhat more hysteresis was observed upon desorption for SPT-CMP2 than was apparent for the other two polymers, which indicates that the material possesses more mesopores. The porous properties of the polymers are summarized in Table 2. SPT-CMP1 shows the highest BET surface area (1631 m^2/g) in the series of three polymers. Thus, it exceeds surface areas obtained for other CMP networks reported previously[16,17,20−22,24,28,35,36] and also exceeds the highest S_{BET} reported for a polymer of intrinsic microporosity (PIM).[6] Figure 3b shows the pore size distribution (PSD) curves for the three polymer networks as calculated using nonlocal density functional theory (NL-DFT). All polymer networks exhibited a micropore diameter centering around 1.1 nm with a shoulder peak at 1.6 nm. Again, the relatively broad PSD curve for all three polymers suggests the presence of both micropores and mesopores. A weak peak at around 7 nm in Figure 3b shows that SPT-CMP2 has many more mesopores than the other two polymers, which is in agreement with the shape of the N_2 isotherms (Figure 3a). The NL-DFT cumulative pore volume plots for the networks (Figure 3c) show that the surface area tracked micropore volume, as observed for other CMPs.[16,17]

Table 2. Porosity Properties and Hydrogen Uptakes for the Polymers

polymer	S_{BET} $[m^2/g]^a$	S_{MICRO} $[m^2/g]^b$	V_{TOTAL} $[cm^3/g]^c$	V_{MICRO} $[cm^3/g]^d$	H_2 uptake [wt %][e]
SPT-CMP1	1631	1108	1.78	0.45	1.72
SPT-CMP2	1601	981	0.98	0.40	1.57
SPT-CMP3	1334	878	1.37	0.36	1.34

[a] Surface area calculated from the N_2 adsorption isotherm using the BET method. [b] Micropore surface area calculated from the N_2 adsorption isotherm using *t*-plot method based on the Harkins−Jura equation. [c] Total pore volume at $P/P_0 = 0.99$. [d] The micropore volume derived using the *t*-plot method. [e] Data were obtained by volumetric measurement at 77.3 K and 1.13 bar.

The permanent porosity in the polymers results from the highly cross-linked and contorted polymer structures due to the introduction of nodes from the ethynyl monomer (for SPT-CMP2 and **3**) and the contorted spiro monomer **2**. We also tried the oxidative polymerization of monomer **1** using a Lewis acid oxidant ($FeCl_3$ in $CHCl_3$), but the resulting insoluble black polymer was nonporous ($S_{BET} = 26\ m^2/g$). The possible reason for the nonporosity of this product could possibly be attributed to the higher conformational flexibility of **1** as discussed above. Thomas[22] and Yu[37] independently reported microporous polymer networks formed using oxidative polymerization of 2,2′,7,7′-tetrakis(2-thienyl)-9,9′-spirobifluoene in which the monomer is highly twisted and contorted due to the fact that the 9,9′-spirobifluorene monomer incorporates a 90° kink in every repeating unit. This prevents the stiff polymer chains from packing efficiently in space, and thus a large accessible free volume and surface area was obtained.[21,22]

Scanning electron micrographs show that the three polymers consist of relatively uniform solid submicrometer spheres (Figure 4). The mesopores in the three polymers can be ascribed mostly to interparticulate porosity that exists between agglomerate primary microgel particles (Figure 4). This kind of mesostructure was not observed for our previous polyaryleneethynylene CMP networks—indeed, those samples were wholly microporous and featureless at this length scale when observed by SEM and TEM.[16,17] This suggests that the phase separation process differs significantly in the SPT-CMP and PAE CMP processes.

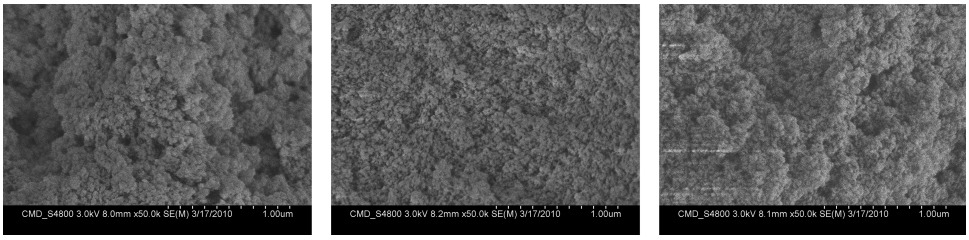

Figure 4. Scanning electron microscope images for the polymer networks of SPT-CMP1 (left), SPT-CMP2 (middle), and SPT-CMP3 (right) (scale bar = 1 μm).

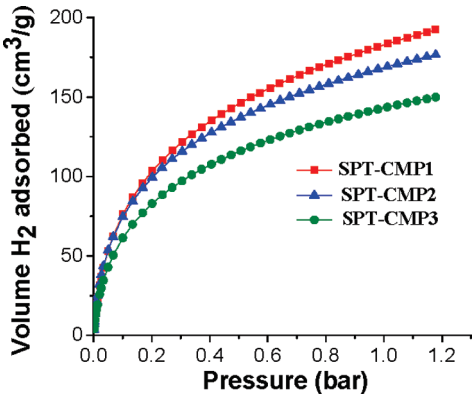

Figure 5. Volumetric H_2 adsorption isotherms for SPT-CMP1−3 up to 1.13 bar at 77.3 K.

The hydrogen sorption properties of the polymers at 77.3 K were investigated by volumetric methods. Figure 5 shows the H_2 adsorption isotherms at 77.3 K up to a maximum H_2 pressure of 1.13 bar. It was found that SPT-CMP1 exhibits a highest H_2 adsorption capacity among the three polymer networks. This can be assigned to the higher micropore surface area and micropore volume observed for SPT-CMP1 (Table 2) since micropores, not mesopores, mostly contribute to the H_2 adsorption at these pressures and temperatures. SPT-CMP1, which has the highest micropore surface area and micropore volume, exhibits the largest H_2 uptake of 192 cm^3/g at 1.13 bar/77.3 K (~1.7 wt %). This is higher than that observed for other CMP networks reported[16,17,19,28] and comparable to the highest of H_2 uptake (1.65 wt %) reported thus far for a polymer of intrinsic microporosity[6] under the same measurement conditions.

Conclusion

We have synthesized a series of contorted conjugated microporous polymer networks by using Sonogashira−Hagihara cross−coupling chemistry from a novel contorted monomer of spiro-bis(2,5-dibromopropylenedioxythiophene). The polymers show enhanced surface areas and exhibit a reversibly adsorb 1.71% hydrogen by mass at 1.13 bar/77 K. While we do not anticipate applications in H_2 storage by simple physisorption, these polymers are highly porous and represent a new class of cross-linked CMP-containing thiophene in the backbone. These findings suggest the possibility for producing composite photovoltaic materials or conducting microporous materials by introducing low band-gap units into the polymer chain.

Acknowledgment. The authors are grateful to EPSRC (EP/F057865/1 and EP/C511794/1), NWDA, and the University of Liverpool for financial support. A.I.C. is a Royal Society Wolfson Merit Award Holder.

Supporting Information Available: Full experimental details for the solid state $^{13}C\{^1H\}$ MAS NMR for the polymers, gas sorption, crystallography, and SEM. This material is available free of charge via the Internet at http://pubs.acs.org.

References and Notes

(1) McKeown, N. B.; Budd, P. M. *Chem. Soc. Rev.* **2006**, *35*, 675–683.
(2) Germain, J.; Frechet, J. M. J.; Svec, F. *Small* **2009**, *5*, 1098–1111.
(3) McKeown, N. B.; Hanif, S.; Msayib, K.; Tattershall, C. E.; Budd, P. M. *Chem. Commun.* **2002**, 2782–2783.
(4) McKeown, N. B.; Makhseed, S.; Budd, P. M. *Chem. Commun.* **2002**, 2780–2781.
(5) McKeown, N. B.; Gahnem, B.; Msayib, K. J.; Budd, P. M.; Tattershall, C. E.; Mahmood, K.; Tan, S.; Book, D.; Langmi, H. W.; Walton, A. *Angew. Chem., Int. Ed.* **2006**, *45*, 1804–1807.
(6) Ghanem, B. S.; Msayib, K. J.; McKeown, N. B.; Harris, K. D. M.; Pan, Z.; Budd, P. M.; Butler, A.; Selbie, J.; Book, D.; Walton, A. *Chem. Commun.* **2007**, 67–69.
(7) Germain, J.; Hradil, J.; Fréchet, J. M. J.; Svec, F. *Chem. Mater.* **2006**, *18*, 4430–4435.
(8) Lee, J. Y.; Wood, C. D.; Bradshaw, D.; Rosseinsky, M. J.; Cooper, A. I. *Chem. Commun.* **2006**, 2670–2672.
(9) Wood, C. D.; Tan, B.; Trewin, A.; Niu, H. J.; Bradshaw, D.; Rosseinsky, M. J.; Khimyak, Y. Z.; Campbell, N. L.; Kirk, R.; Stockel, E.; Cooper, A. I. *Chem. Mater.* **2007**, *19*, 2034–2048.
(10) Kuhn, P.; Antonietti, M.; Thomas, A. *Angew. Chem., Int. Ed.* **2008**, *47*, 3450–3453.
(11) Côté, A. P.; Benin, A. I.; Ockwig, N. W.; O'Keeffe, M.; Matzger, A. J.; Yaghi, O. M. *Science* **2005**, *310*, 1166–1170.
(12) El-Kaderi, H. M.; Hunt, J. R.; Mendoza-Cortes, J. L.; Côté, A. P.; Taylor, R. E.; O'Keeffe, M.; Yaghi, O. M. *Science* **2007**, *316*, 268–272.
(13) Germain, J.; Frechet, J. M. J.; Svec, F. *J. Mater. Chem.* **2007**, *17*, 4989–4997.
(14) Ghanem, B. S.; McKeown, N. B.; Budd, P. M.; Al-Harbi, N. M.; Fritsch, D.; Heinrich, K.; Starannikova, L.; Tokarev, A.; Yampolskii, Y. *Macromolecules* **2009**, *42*, 7881–7888.
(15) Farha, O. K.; Spokoyny, A. M.; Hauser, B. G.; Bae, Y. S.; Brown, S. E.; Snurr, R. Q.; Mirkin, C. A.; Hupp, J. T. *Chem. Mater.* **2009**, *21*, 3033–3035.
(16) Jiang, J. X.; Su, F.; Trewin, A.; Wood, C. D.; Campbell, N. L.; Niu, H.; Dickinson, C.; Ganin, A. Y.; Rosseinsky, M. J.; Khimyak, Y. Z.; Cooper, A. I. *Angew. Chem., Int. Ed.* **2007**, *46*, 8574–8578.
(17) Jiang, J. X.; Su, F.; Trewin, A.; Wood, C. D.; Niu, H.; Jones, J. T. A.; Khimyak, Y. Z.; Cooper, A. I. *J. Am. Chem. Soc.* **2008**, *130*, 7710–7720.
(18) Cooper, A. I. *Adv. Mater.* **2009**, *21*, 1291–1295.
(19) Jiang, J. X.; Su, F.; Niu, H.; Wood, C. D.; Campbell, N. L.; Khimyak, Y. Z.; Cooper, A. I. *Chem. Commun.* **2008**, 486–488.
(20) Dawson, R.; Su, F. B.; Niu, H. J.; Wood, C. D.; Jones, J. T. A.; Khimyak, Y. Z.; Cooper, A. I. *Macromolecules* **2008**, *41*, 1591–1593.
(21) Weber, J.; Thomas, A. *J. Am. Chem. Soc.* **2008**, *130*, 6334–6335.
(22) Schmidt, J.; Weber, J.; Epping, J. D.; Antonietti, M.; Thomas, A. *Adv. Mater.* **2009**, *21*, 702–705.
(23) Kobayashi, N.; Kijima, M. *J. Mater. Chem.* **2007**, *17*, 4289–4296.
(24) Schmidt, J.; Werner, M.; Thomas, A. *Macromolecules* **2009**, *42*, 4426–4429.
(25) Ben, T.; Ren, H.; Ma, S. Q.; Cao, D. P.; Lan, J. H.; Jing, X. F.; Wang, W. C.; Xu, J.; Deng, F.; Simmons, J. M.; Qiu, S. L.; Zhu, G. S. *Angew. Chem., Int. Ed.* **2009**, *48*, 9457–9460.
(26) Trewin, A.; Cooper, A. I. *Angew. Chem., Int. Ed.* **2010**, *49*, 1533–1535.
(27) Chen, L.; Honsho, Y.; Seki, S.; Jiang, D. L. *J. Am. Chem. Soc.* **2010**, *132*, 6742–6748.

(28) Dawson, R.; Laybourn, A.; Clowes, R.; Khimyak, Y. Z.; Adams, D. J.; Cooper, A. I. *Macromolecules* **2009**, *42*, 8809–8816.
(29) Roncali, J. *Macromol. Rapid Commun.* **2007**, *28*, 1761–1775.
(30) Chen, J. W.; Cao, Y. *Acc. Chem. Res.* **2009**, *42*, 1709–1718.
(31) Piron, F.; Leriche, P.; Mabon, G.; Grosu, I.; Roncali, J. *Electrochem. Commun.* **2008**, *10*, 1427–1430.
(32) Groenendaal, B. L.; Jonas, F.; Freitag, D.; Pielartzik, H.; Reynolds, J. R. *Adv. Mater.* **2000**, *12*, 481–494.
(33) Groenendaal, L.; Zotti, G.; Aubert, P. H.; Waybright, S. M.; Reynolds, J. R. *Adv. Mater.* **2003**, *15*, 855–879.
(34) Reeves, B. D.; Thompson, B. C.; Abboud, K. A.; Smart, B. E.; Reynolds, J. R. *Adv. Mater.* **2002**, *14*, 717–719.
(35) Jiang, J. X.; Trewin, A.; Su, F. B.; Wood, C. D.; Niu, H. J.; Jones, J. T. A.; Khimyak, Y. Z.; Cooper, A. I. *Macromolecules* **2009**, *42*, 2658–2666.
(36) Stockel, E.; Wu, X. F.; Trewin, A.; Wood, C. D.; Clowes, R.; Campbell, N. L.; Jones, J. T. A.; Khimyak, Y. Z.; Adams, D. J.; Cooper, A. I. *Chem. Commun.* **2009**, 212–214.
(37) Yuan, S. W.; Kirklin, S.; Dorney, B.; Liu, D. J.; Yu, L. P. *Macromolecules* **2009**, *42*, 1554–1559.